Applied Mathematical Modelling 37 (2013) 4360–4370

Contents lists available at SciVerse ScienceDirect

Applied Mathematical Modelling

journal homepage: www.elsevier.com/locate/apm

Modeling and analysis of distributed electromagnetic oscillators for broadband vibration attenuation and concurrent energy harvesting

Ryan L. Harne *

Department of Mechanical Engineering, Virginia Polytechnic Institute and State University, 151 Durham Hall (MC 0238), Blacksburg, VA 24061, USA

ARTICLE INFO

Article history:
Received 3 March 2012
Received in revised form 8 July 2012
Accepted 18 September 2012
Available online 27 September 2012

Keywords:
Passive vibration control
Energy harvesting
Electromagnetism

ABSTRACT

Many energy harvesting devices employ dynamics ascribed to the classical vibration absorber. Conventional models suggest that when host structural motion excites the harvesters at resonance, maximum electrical power output is achieved. As the harvesters become inertially substantial relative to the structure, this condition no longer holds since the electro-elastic response of the harvester is coupled to the structural vibration. In this regime, the devices become true vibration absorbers that alter the structural oscillations which may consequently affect energy harvesting capability. Distributions of point oscillators have been considered as broadband vibration control treatments making it natural to consider the potential for energy harvesting devices to serve this end. This paper presents an analysis of distributed single- and two-degree-of-freedom, linear electromagnetic oscillators attached to a harmonically excited panel. The coupled Euler–Lagrange equations of motion are solved and the simultaneous goals of vibration attenuation of the host panel and harvested electrical power are computed for several scenarios. It is found that design parameters optimizing the individual goals occur in relative proximity such that small compromises need to be made in order to achieve both ends reasonably well, particularly in regards to the overall mass added to the structure.

1. Introduction

The interest in converting ambient vibrational energy into useful electrical power has led to a broad range of devices employing electromechanical coupling. Whether embodied as cantilevered specimens [1–3], mass-spring oscillators [4–7], or surface-attached treatments [8,9], the devices are excited by the host structural vibration and external circuits are utilized to quantify the net electrical power output. A frequent assumption in the fundamental analysis of basic oscillator-type harvesters is that the devices are excited by way of base vibration [10–14]. This is appropriate in light of some anticipated MEMS applications. But as energy harvesting prototypes become inertially substantial relative to the main structure, this mathematical model is no longer accurate.

Damping induced via piezoelectric energy harvesting has been studied and exploited as a vibration control mechanism [15–17]. The first-order dissipation is in contrast to the present focus of second-order dynamic coupling in which a primary mass-spring system is acted upon by an auxiliary electromechanical mass-spring system. The concept of "dynamic magnifier" harvester—a harvester beam attached to the free end of a structural cantilevered beam—adopts this perspective of a critical dynamic coupling between energy harvester and the host structure [18–20]. Additionally, a recent study by Tang and Zuo [21] investigated dual-mass harvester designs. The electro-dynamic coupling is a two degree-of-freedom (2DOF)

* Tel.: +1 540 231 4162.
E-mail address: rharne@vt.edu

0307-904X/$ - see front matter © 2012 Elsevier Inc. All rights reserved.
http://dx.doi.org/10.1016/j.apm.2012.09.047

mechanical model with an additional DOF resulting from the external circuit potential. From this perspective, rather than achieving vibration damping while harvesting energy, the second-order influence may be regarded as achieving vibration control with energy harvesting. This equalizes the importance of both goals but does not necessitate their concurrent success.

Other recent works have taken this point of view in modeling and constructing experimental samples of vibration absorbers having electromechanical members so as to ideally serve both objectives. For instance, electromechanical skyscraper tuned-mass-dampers required to attenuate wind- or seismic-induced vibration appear a prime application for large-scale energy harvesting [22,23]. Another study considers the control of lightweight structural panels with distributed piezoelectric vibration control devices which benefit from the inherent damping of the piezoelectric polymer while still providing viable electrical output when excited near resonance [24].

The use of undamped oscillator arrays to passively attenuate structural vibrations has been widely studied in the language of the "structural fuzzy" [25–27]. This concept reduces the DOF in modeling by considering the oscillator array as being a distributed impedance. Other work has similarly studied numerous attached mass-spring systems to attenuate structural vibrations though retaining the full multi-DOF modeling description [28,29], essentially the same aim in analysis only with increased computational expense. Zuo and Nayfeh [29] specifically focus on the optimization of stiffness and damping parameters for the attached oscillator array to achieve global vibration reduction.

Employing arrays of electromechanical oscillators—equally "energy harvesters"—may have the same potential for global vibration control. Furthermore, the damping mechanism of such devices is the conversion of the "absorbed" mechanical energy into electrical power, dependent on the strength of electromechanical coupling. The achievement of both energy harvesting and vibration control are therefore weighed as equally important objectives in the present study.

Practical embodiments of energy harvesting devices regularly take the form of cantilevered piezoelectric samples or point mass-spring electromagnetic devices, as referenced earlier. Though some study has, indeed, considered the use of multiple cantilevered beams in passively attenuating the vibrations of a host beam [28], the present analysis will be concerned with electromagnetic point oscillators given their practical similarity to the classical 1DOF tuned-mass-damper.

The host or primary structure of present interest is a conventional, rectangular panel. Such structural panels are ubiquitous (aerospace and maritime vehicles, building panels, windows, for example) and are primarily excited in their lowest order modes. A conventional energy harvesting analysis may presume the devices to be best positioned at the lowest mode antinode so as to be most excited, thus harvesting the most electrical power and also justifying a simplification of the modeling to focus on single-mode excitation (*i.e.* SDOF assumptions). However, the centralized positioning of the oscillators does not necessarily achieve optimum global vibration control of the structure. Thus, a distributed panel serves as an important case study for evaluating the simultaneous achievement of vibration control and energy harvesting using arrays of electromechanical oscillators.

This paper derives the governing equations for the coupled electro–elastic dynamics of a simply-supported rectangular panel to which a number of electromagnetically (E–M) coupled SDOF or 2DOF oscillators are attached. The E–M mass-spring-dampers are attached to external circuits and the coupled Euler–Lagrange governing equations are solved simultaneously to determine the electric and mechanical dynamics. Metrics of global vibration suppression and maximum energy harvested are utilized and a number of scenarios are considered: single oscillators, random distributions of oscillators and the effects of oscillator array number. Design parameter sets to optimize the individual goals are found to occur relatively close together. This indicates small compromises in both objectives need to be accepted to satisfy both ends relatively well.

2. Model formulation

A thin, simply-supported rectangular panel is considered, to which N_p SDOF or 2DOF mass-spring-dampers have been attached at positions (x_i^p, y_i^p), Fig. 1. The host panel is excited by N_f out-of-plane harmonic point forces, $f_i(x_i^f, y_i^f, t)$. The attached

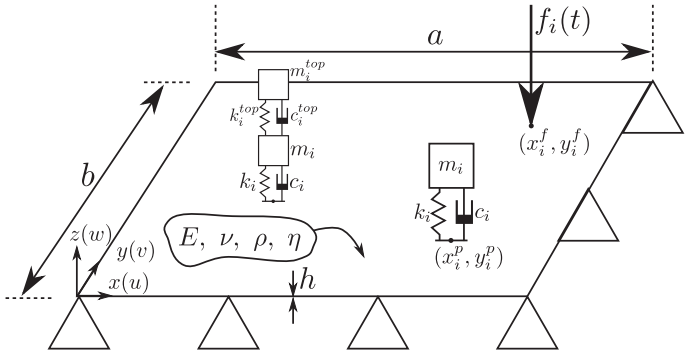

Fig. 1. Mechanical geometry of the present analysis.

oscillators exhibit an electromagnetic coupling as, in one conceivable embodiment, the magnetic mass, m_i, moves along the axis of a conductive coil inducing a flow of electrical current through an external circuit (Fig. 2) [7,30]. In the case of the 2DOF oscillators, it is assumed that only one of the oscillating sub-systems exhibits electromagnetic coupling. This embodiment represents a similar idea in the literature of the "dynamic magnifier" harvester in which case a piezoelectric beam harvester is attached to a purely structural beam, the combination of the two degrees-of-freedom leading to increased power harvesting [19,20]. In the present analysis, the oscillator spring deformation is assumed to remain linear.

The Lagrangian of the system is

$$L = T - V + W_m. \tag{1}$$

The total kinetic energy, T, is the sum of the contributions from the host panel and the attached oscillators

$$T = \frac{1}{2}\rho \int_\Omega \dot{\mathbf{u}}^t \dot{\mathbf{u}} \mathrm{d}\Omega + \frac{1}{2}\sum_{i=1}^{N_p} m_i \left[\dot{w}(x_i^p, y_i^p) + \dot{z}_i\right]^2 + \frac{1}{2}\sum_{i=1}^{N_p} m_i^{top} \left[\dot{w}(x_i^p, y_i^p) + \dot{z}_i + \dot{z}_i^{top}\right]^2, \tag{2}$$

where the displacements of the panel are $\mathbf{u} = [u(x,y,t)\ \ v(x,y,t)\ \ w(x,y,t)]^t$; ρ is the panel mass density; m_i is the mass of the ith mass-spring-damper attached to the panel at (x_i^p, y_i^p); z_i is the relative displacement between the ith mass-spring-damper sub-system and the panel; and where z_i^{top} represents the relative displacement between the top oscillator, of mass m_i^{top}, and the bottom oscillator of the 2DOF system. The time derivative is denoted by $\dot{()}$ and $()^t$ denotes the matrix transpose operator.

The total potential energy, V, is

$$V = \frac{1}{2}\int_\Omega \epsilon^t \tau \epsilon \mathrm{d}\Omega + \frac{1}{2}\sum_{i=1}^{N_p} k_i z_i^2 + \frac{1}{2}\sum_{i=1}^{N_p} k_i^{top} \left(z_i^{top}\right)^2, \tag{3}$$

where ϵ is the strain tensor of the panel; τ is the stiffness matrix of the panel; k_i is the spring constant of the bottom oscillator; and k_i^{top} is the spring constant of the top oscillator.

The electromagnetic energy in the coils, W_m, is

$$W_m = \frac{1}{2}\sum_{i=1}^{N_p} \left[L_i \dot{q}_i^2 + T_i \dot{q}_i z_i\right], \tag{4}$$

where L_i is the internal inductance of the coils of the ith oscillator; q_i is the charge passing through the coils; and $T_i = B_i l_i$ is linear transducer constant for the oscillator, calculated as the product of the magnetic flux density, B_i, and the length of the conductive coils l_i. If the top mass of a 2DOF oscillator is electromagnetically-coupled, one replaces the term z_i in Eq. (4) with z_i^{top}. A linear transducer constant is assumed for simplification in the present analysis; this has been shown to be a reasonable approximation so long as the magnet remains within the length of the exterior coil [30].

The dissipation function for the coupled system is the sum of the contributions of mechanical damping in the panel and of attached circuitry to the electromagnetic oscillators. It is here assumed that the external circuits are composed of resistive loads, R_i, such that the total dissipation function is

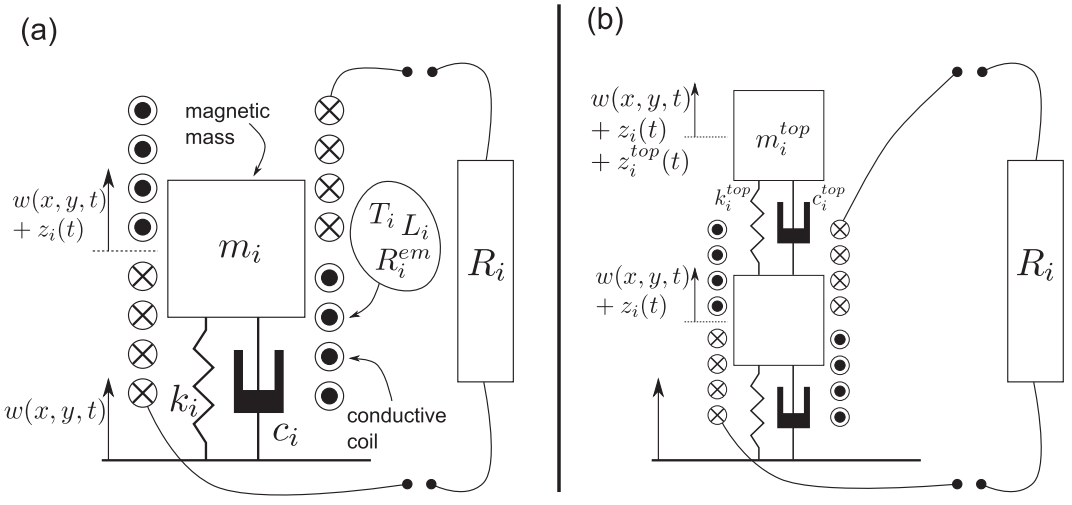

Fig. 2. Schematics of (a) SDOF E–M oscillators and (b) 2DOF oscillators, here showing electromagnetic coupling for the bottom oscillator sub-system.

$$D = \frac{1}{2}c\int_{\Omega}\dot{\mathbf{u}}^t\dot{\mathbf{u}}\mathrm{d}\Omega + \frac{1}{2}\sum_{i=1}^{N_p}c_i\dot{z}_i^2 + \frac{1}{2}\sum_{i=1}^{N_p}c_i^{top}\left(\dot{z}_i^{top}\right)^2 + \frac{1}{2}\sum_{i=1}^{N_p}\left(R_i + R_i^{em}\right)\dot{q}_i^2, \tag{5}$$

where c is the viscous damping coefficient of the panel; c_i is the damping coefficient of the bottom oscillator; c_i^{top} is the damping coefficient of the top oscillator; and R_i^{em} is the resistance of the conductive coil. The damping ratio of the oscillators is defined as $\zeta_i = c_i/2\sqrt{m_i k_i}$. In the present study, $c_i = c_i^{top}$.

The Euler–Lagrange governing equations for the coupled system are

$$\begin{aligned}
&\frac{\mathrm{d}}{\mathrm{d}t}\left[\frac{\partial L}{\partial\dot{\mathbf{u}}}\right] + \frac{\partial D}{\partial\dot{\mathbf{u}}} - \frac{\partial L}{\partial\mathbf{u}} = \mathbf{F},\\
&\frac{\mathrm{d}}{\mathrm{d}t}\left[\frac{\partial L}{\partial\dot{z}_i}\right] + \frac{\partial D}{\partial\dot{z}_i} - \frac{\partial L}{\partial z_i} = 0,\\
&\frac{\mathrm{d}}{\mathrm{d}t}\left[\frac{\partial L}{\partial\dot{z}_i^{top}}\right] + \frac{\partial D}{\partial\dot{z}_i^{top}} - \frac{\partial L}{\partial z_i^{top}} = 0,\\
&\frac{\mathrm{d}}{\mathrm{d}t}\left[\frac{\partial L}{\partial\dot{q}_i}\right] + \frac{\partial D}{\partial\dot{q}_i} - \frac{\partial L}{\partial q_i} = 0,
\end{aligned} \tag{6}$$

where $\mathbf{F}(t) = \sum_{i=1}^{N_f}\mathbf{f}_i(\mathbf{x}_i^f, t)\mathbf{u}(\mathbf{x}_i^f)$ are the generalized forces.

For the thin, isotropic panel of interest and considering harmonic excitation:

$$\mathbf{u} = \begin{bmatrix} -z\frac{\partial w(x,y,\omega)}{\partial x}\\ -z\frac{\partial w(x,y,\omega)}{\partial y}\\ w(x,y,\omega)\end{bmatrix} \qquad \epsilon = \begin{bmatrix}\epsilon_x\\ \epsilon_y\\ 2\epsilon_{xy}\end{bmatrix} \qquad \tau = \begin{bmatrix}\frac{E}{1-\nu^2} & \frac{\nu E}{1-\nu^2} & 0\\ \frac{\nu E}{1-\nu^2} & \frac{E}{1-\nu^2} & 0\\ 0 & 0 & \frac{E}{2(1+\nu)}\end{bmatrix}, \tag{7}$$

where E is the Young's modulus and ν is the Poisson's ratio. A Ritz method solution form for the panel displacement is assumed:

$$w(x,y,\omega) = \sum_{n=1}^{N}a_n(\omega)\Psi_n(x,y), \tag{8}$$

where $\mathbf{a}(\omega) = [a_1(\omega)\ a_2(\omega)\cdots a_N(\omega)]^t$ are the N generalized co-ordinates and $\Psi(x,y) = [\Psi_1(x,y)\ \Psi_2(x,y)\cdots\Psi_N(x,y)]$ the admissible trial functions of the panel out-of-plane displacement. Substituting the above components into the Euler–Lagrange Eq. (6)(a–d) and assuming the bottom oscillator is electromagnetically coupled yields

$$\begin{aligned}
&\left[-\omega^2(M_{mn} + H_{mn} + G_{mn}) + j\omega C_{mn} + K_{mn}\right]a_m(\omega)\\
&-\omega^2\left[\sum_{i=1}^{N_p}m_i\Psi_m(x_i^p, y_i^p)z_i(\omega) + \sum_{i=1}^{N_p}m_i^{top}\Psi_m(x_i^p, y_i^p)z_i^{top}(\omega)\right] = F_m(\omega) \quad m = 1,2,\ldots,N;\ n = 1,2,\ldots,N,
\end{aligned} \tag{9}$$

$$-\omega^2 m_i\sum_{m=1}^{N}\Psi_m(x_i^p, y_i^p)a_m(\omega) + \left[-\omega^2 m_i + j\omega c_i + k_i\right]z_i(\omega) - \omega^2 m_i^{top}z_i^{top}(\omega) - j\omega T_i q_i(\omega) = 0 \quad i = 1,2,\ldots,N_p, \tag{10}$$

$$-\omega^2 m_i^{top}\sum_{m=1}^{N}\Psi_m(x_i^p, y_i^p)a_m(\omega) - \omega^2 m_i z_i(\omega) + \left[-\omega^2 m_i^{top} + j\omega c_i^{top} + k_i^{top}\right]z_i^{top}(\omega) = 0 \quad i = 1,2,\ldots,N_p, \tag{11}$$

$$j\omega T_i z_i(\omega) + \left[-\omega^2 L_i + j\omega\left(R_i + R_i^{em}\right)\right]q_i(\omega) = 0 \quad i = 1,2,\ldots,N_p. \tag{12}$$

In the event that the top oscillator is electromagnetically coupled, the term $-j\omega T_i q_i(\omega)$ of Eq. (10) is transferred to Eq. (11) and the term z_i in Eq. (12) is replaced with z_i^{top}. The following are specified

$$M_{mn} = \rho h\int_0^a\int_0^b\left[\Psi_m\Psi_n + \frac{h^2}{12}\left(\frac{\partial\Psi_m}{\partial x}\frac{\partial\Psi_n}{\partial x} + \frac{\partial\Psi_m}{\partial y}\frac{\partial\Psi_n}{\partial y}\right)\right]\mathrm{d}x\mathrm{d}y, \tag{13}$$

$$K_{mn} = \frac{Eh^3}{12(1-\nu^2)}\int_0^a\int_0^b\left[\frac{\partial^2\Psi_m}{\partial x^2}\frac{\partial^2\Psi_n}{\partial x^2} + \nu\left[\frac{\partial^2\Psi_m}{\partial x^2}\frac{\partial^2\Psi_n}{\partial y^2} + \frac{\partial^2\Psi_m}{\partial y^2}\frac{\partial^2\Psi_n}{\partial x^2}\right] + \frac{\partial^2\Psi_m}{\partial y^2}\frac{\partial^2\Psi_n}{\partial y^2} + 2(1-\nu)\frac{\partial^2\Psi_m}{\partial x\partial y}\frac{\partial^2\Psi_n}{\partial x\partial y}\right]\mathrm{d}x\mathrm{d}y, \tag{14}$$

$$C_{mn} = \alpha M_{mn} + \beta K_{mn}, \tag{15}$$

$$H_{mn} = \sum_{i=1}^{N_p} m_i \Psi_m(x_i^p, y_i^p) \Psi_n(x_i^p, y_i^p), \tag{16}$$

$$G_{mn} = \sum_{i=1}^{N_p} m_i^{top} \Psi_m(x_i^p, y_i^p) \Psi_n(x_i^p, y_i^p), \tag{17}$$

$$F_m(\omega) = \sum_{i=1}^{N_f} f_i(x_i^f, y_i^f, \omega) \Psi_m(x_i^f, y_i^f). \tag{18}$$

Eqs. (9)–(12) are composed of $N + 2N_p$ generalized co-ordinates for the system employing SDOF oscillators and $N + 3N_p$ co-ordinates for 2DOF oscillators. The mass ratio is defined as

$$\mu = \frac{\sum_{i=1}^{N_p} [m_i + m_i^{top}]}{abh\rho}. \tag{19}$$

As a metric to evaluate the global vibration levels of the panel, the spatial average mean-square out-of-plane velocity is computed as

$$\langle \dot{w}(\omega) \rangle^2 = \frac{\omega^2}{2ab} a_m^*(\omega) a_n(\omega) \int_0^a \int_0^b \Psi_m(x,y) \Psi_n(x,y) \mathrm{d}x\mathrm{d}y \quad m = 1,2,\ldots,N;\ n = 1,2,\ldots,N, \tag{20}$$

where $()^*$ denotes the complex conjugate. Average mean-square velocity over a bandwidth of frequencies, *BW*, is the ensemble average of the values:

$$\langle \underline{\dot{w}} \rangle^2 = \frac{1}{BW} \sum_{r=1}^{BW} \langle \dot{w}(\omega_r) \rangle^2. \tag{21}$$

The attenuation of the panel vibration from the untreated levels is expressed as the difference

$$\Delta \langle \underline{\dot{w}} \rangle^2 = \langle \underline{\dot{w}} \rangle^2_{withoscillators} - \langle \underline{\dot{w}} \rangle^2_{untreated}. \tag{22}$$

The author notes that other vibration control metrics could be utilized which average over the surface of the panel, *e.g.* mean-square acceleration, but expressions exist in the literature for computing radiated sound fields from rectangular panels from measurements of surface velocity [31,32]. This gives the mean-square velocity metric a tangible, though indirect, connection to sound radiation control, which is also of practical use.

The current through the ith load resistance, R_i, is determined by $i_i(\omega) = \dot{q}_i(\omega)$. The voltage over the resistance is therefore computed as $v_i(\omega) = i_i(\omega) R_i$ and the average power in the circuit is $P_i(\omega) = |v_i(\omega)|^2 / 2R_i$. The maximum power achieved over the desired bandwidth is the metric of interest for energy harvesting.

The following sections solve the systems of equations, Eqs. (9)–(12), using MATLAB for a variety of examples of device number, placement and configuration. Performance metrics of comparison are the maximum power for energy harvesting evaluation and the attenuation of panel vibration $\Delta \langle \underline{\dot{w}} \rangle^2$ for vibration control. The variables of interest to be modified are presently the oscillator treatment mass ratio μ and the load resistance of the harvesting circuit R_1. Expanding the work to study the effects of varying electrical or electromechanical parameters is left to further investigation.

3. One centrally-located oscillator

To initially evaluate the simultaneous aims of vibration suppression and energy harvesting from the same device, consider a single electromagnetic oscillator positioned at the center of the panel. Geometric and material properties of the system are provided in Table 1. Damping of the panel is included by means of an isotropic loss factor, η, such that in Eq. (15), $\alpha = 0$ and $\beta = \eta/\omega$. The oscillators are either a SDOF device, a 2DOF device with E–M coupling on the bottom sub-system or a 2DOF device with coupling on the top oscillating mass. In the event of the 2DOF device, it was assumed that the total mass ratio, μ, was split with 70% of the mass as the bottom oscillator and 30% of the mass as the top oscillator; this selection is representative of the relative scales in the literature studying the dynamic magnifier harvester concept [19,20]. Properties of the oscillator electrical and electromechanical characteristics are provided in Table 2 and are representative of properties elsewhere used in literature [11].

Table 1
Panel specifications.

a (mm)	b (mm)	h (mm)	E (Pa)	ν	ρ (kg/m^3)	η	(x_1^f, y_1^f) (mm)
600	400	2	7.1e10	0.3	2100	1e−3	(100,100)

Table 2
Oscillator specifications.

ζ_1	T_1 (T·m)	L_1 (μH)	R_1^{em} (Ω)	(x_1^p, y_1^p) (mm)
1e−2	10	100	5	(300,200)

The SDOF oscillators are tuned to have a natural frequency of 50 Hz; as such, the individual mass, m_i, and spring constant, k_i, change with each run of the model as μ is modified. For the 2DOF oscillators, the bottom oscillator natural frequency is maintained at $\sqrt{k_i/m_i}/2\pi$ =61 Hz, while for the top sub-system $\sqrt{k_i^{top}/m_i^{top}}/2\pi = 143$ Hz. Collectively, the 2DOF oscillator natural frequencies become 50 Hz and 174 Hz [33]. These two frequencies are close to the (1,1) and (3,1) modal resonance frequencies of the panel, 50 and 173 Hz, respectively, and are therefore both capable of being attenuated by the 2DOF device.

Numerical simulations of the forced response of the panel were computed from 1–300 Hz in 1 Hz increments. This bandwidth contains the first 7 modes of the panel: 50 Hz (1,1); 96 Hz (2,1); 154 Hz (1,2); 173 Hz (3,1); 200 Hz (2,2); 276 Hz (3,2); and 280 Hz (4,1). The metrics of maximum power, Eq. (21)(b), and reduction in the panel mean-square velocity, Eq. (22), were computed for a range of μ and R_1.

Fig. 3 plots the metrics of vibration suppression (top row) and energy harvesting (bottom row) for the case of adding the SDOF oscillator (first column), 2DOF oscillator with bottom E–M coupling (second column) and 2DOF oscillator with top E–M coupling (third column). Unsurprisingly, maximum vibration attenuation is achieved by greater addition of mass, to a point, as well as the least load resistances. The SDOF oscillator is most capable of panel vibration control but as the mass of the oscillator approaches that of the panel, $\mu \to 1$, the coupled dynamics become detrimental to suppressing the structural vibration. It is found that the optimum design parameters for vibration control occur for the SDOF oscillator at $R_1 = R_{em}$, the coil resistance, and $\mu \approx 0.1$. In terms of the electrical circuit, this selection of R_1 is a case of impedance-matching so as to maximize the flow of current across the resistor to achieve greatest circuit dissipation.

From the bottom row of Fig. 3, maximized output power is found to be achieved for slightly different selection of μ and R_1 as for maximum vibration attenuation. For the SDOF oscillator the greatest power is generated for $\mu = 0.022$ and $R_1 = 44.6\Omega : P_1 = 10.4$ μW. It is interesting to observe that the metric of electrical power is comparatively insensitive to changes in μ and R_1, providing for a practical versatility in achieving both passive vibration control and power harvesting.

Neither of the two cases of 2DOF oscillators achieve this magnitude of power output. Though the increased dynamic complexity of the device may help explain why it is less useful in generating significant electrical power, this same feature might also be argued as a benefit. The second natural frequency of the device, 174 Hz, was designed so as to match a symmetric

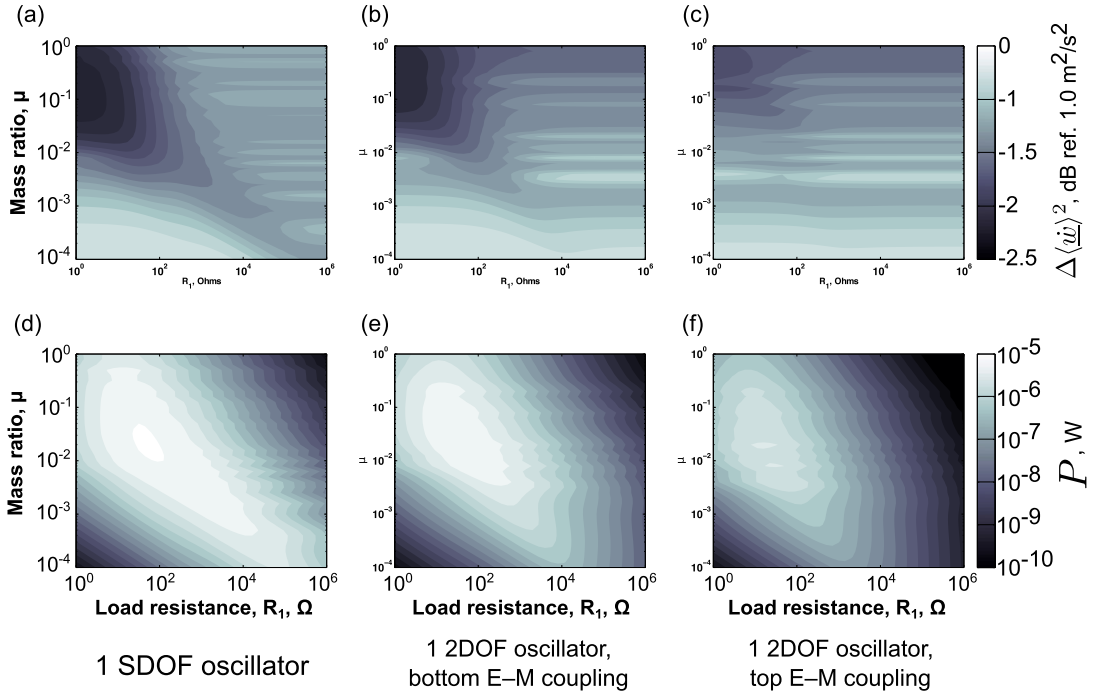

Fig. 3. Vibration suppression for case of the panel having a (a) SDOF oscillator, (b) 2DOF oscillator with bottom E–M coupling and (c) 2DOF oscillator having top E–M coupling. Energy harvesting for panel having a (d) SDOF oscillator, (e) 2DOF oscillator with bottom coupling and (f) 2DOF oscillator with top coupling.

mode shape of the panel, 173 Hz; thus, whether operating at 50 Hz or 174 Hz, the device was intended to be of greater electrical and mechanical benefit than the SDOF device which is principally useful at 50 Hz. However, it appears that the presence of the non-E–M-coupled mass in the 2DOF oscillator is ultimately a detriment to the generation of electrical power in that it serves to reduce the net power input into the component which is coupled to the external circuit. This loss of authority is also seen in Fig. 3(b) and (c) for vibration control purposes, initially suggesting multi DOF oscillators or harvesters are a poor design.

Fig. 4(a) presents the panel average mean-square velocity before and after application of the SDOF oscillator having the optimized parameters to achieve overall vibration control and maximum power harvesting. Like classical vibration absorbers, the dynamic coupling between E–M oscillator and panel yield split resonances around the original panel resonance of 50 Hz. The benefit of the additional mass of the oscillator having parameters optimized for vibration control is that it assists in attenuating the (3,1) mode at 173 Hz, improving global attenuation. Overall, however, there is a minor difference in the net vibration attenuation achieved between the two optimized parameter sets: Fig. 3 predicts a −2.4 dB net attenuation and −1.7 dB attenuation for the vibration control and energy harvesting parameter sets, respectively. (Note that the greater vibrational energy in this case study occurs at the (2,1) mode at 96 Hz; therefore the substantial attenuation of the (1,1) mode becomes somewhat hidden by this fact when determining the ensemble average of mean-square velocity).

Fig. 4(b) plots the output electrical power for the two optimized parameter sets for the SDOF oscillator. The mechanical dynamic coupling between the attached device and the excited panel produce the split resonances which thereafter are the frequencies at which the oscillator outputs greatest electrical power. This is a feature not presently considered in most energy harvesting analyses which regularly predict maximum power to be achieved at the harvester resonance. However, such studies would not take into account the resonant coupling between the harvester and the host structure in the manner presently considered. The study by Tang and Zuo [21] recently observed this opportunity for achieving greater electrical power via dynamic coupling in relation to a "dual-mass" harvester; in the context of the present work, this is the relation between the host panel and the SDOF E–M oscillator.

4. Randomly positioned oscillators

In practice, it is well-known that a single vibration absorber device will have little authority at passively controlling the broadband vibration of a distributed structure. Thus, a solution may be to apply a greater number of absorbers over the structural surface having total mass satisfying a designated limit on μ. This is the aim of a variety of numerical and

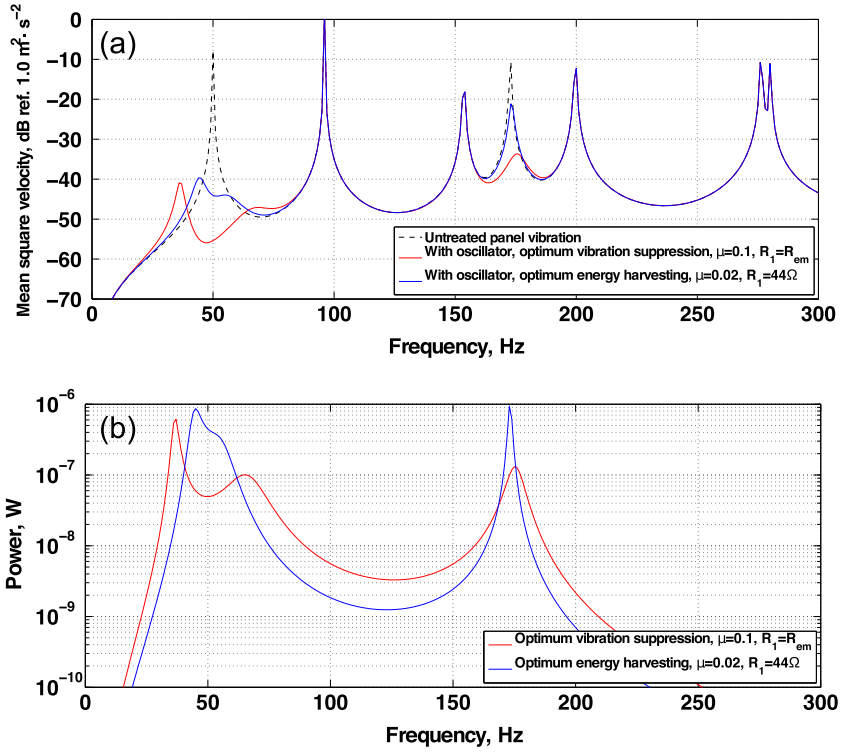

Fig. 4. (a) Panel average mean-square velocity before and after attachment of SDOF oscillator have optimized design parameters for the two goals of vibration control and energy harvesting. (b) Output electrical power for the oscillators for these optimized parameters.

experimental research aimed at achieving maximum vibration control of a main structure by employing numerous damped or undamped mass-spring systems [25–28].

The simulations were then evaluated using a random distribution of 15 oscillators, having positions indicated as in Fig. 5. The only restriction on the position of the oscillators was that the random distribution be confined from $a/6 < x_i^p < 5a/6$ and $b/6 < y_i^p < 5b/6$. Since the panel was supported at the edges, oscillators placed close to the panel extremities would be of little use since they would be poorly excited.

The range of μ and R_i was again varied, maintaining the same R_i for each oscillator. The natural frequencies of the devices were the same as in Section 3. The mass of the oscillators was evenly distributed, such that $m_i = abh\rho\mu/15$, and the same 70/30 bottom/top split of mass was chosen for the 2DOF oscillators. Since the devices were positioned as shown in Fig. 5 and are no longer guaranteed to fall on a nodal line of asymmetric panel modes, they were capable of attenuating vibration over the full 1–300 Hz bandwidth of interest, despite being tuned to just 50 Hz or 50 and 174 Hz for the 2DOF oscillators.

Fig. 6 plots the results of varying μ and R_i in achieving reduction in panel average mean-square velocity and in generating electrical power. The energy harvesting metric is computed as the sum of the maximum powers generated by each oscillator. Unlike with a single oscillator, using numerous devices is beneficial in reducing the panel vibration almost exclusively by employing greater mass ratios although the net reduction in vibration is also much greater. The compromise between total added mass of oscillators and achieving global vibration control is one of the factors considered in past research [29] and is regularly one of the most important practical features in the employment of vibration absorbers in transportation systems for which added mass comes at the cost of extra propulsive power. However, in the present study, it is found that when reducing the added mass, *e.g.* from $\mu = 0.1$ to 0.01, the ability to modify the harvesting circuit load resistance, R_1, serves as a means by which to maximize global vibration control for the given μ. This is verification that in the present context energy harvesting devices are analogous to electromechanical vibration absorbers.

As before, the 2DOF oscillators are uniformly less useful in suppressing panel vibration than the SDOF devices. Multi DOF tuned-mass-dampers have been studied sporadically in the literature [34–36], but it appears that this concept was successfully employed in practice only in conjunction with robust optimization methods [37]. From this perspective, it is not surprising that the 2DOF oscillators are less useful than the SDOF devices, the latter being the more common means by which to attenuate multiple structural modes when using resonant absorbers.

Fig. 6(d)–(f) show that the optimum μ has shifted towards somewhat increased overall mass, though the optimum R_1 is unchanged. Yet, this metric is still found to be much less sensitive in changing μ and R_1 as compared with the vibration control metric. Once again, it may be said that small compromise may be made to achieve both goals well since optimal parameters μ and R_1 are found to be in close proximity. Also as before, the 2DOF oscillators are the inferior embodiment of energy harvesting devices, at least in the event that only one of the masses is electromagnetically coupled to the harvesting circuit.

On the whole, however, the net maximum power from the SDOF oscillators does not scale simply by the array size. In other words, the results from Fig. 3(d) found that the single SDOF oscillator achieved maximum power output of 10.4 μW but Fig. 6(d) shows the 15 oscillators do not achieve 15 times this amount (156 μW) but instead only a maximum of 26.1 μW. This is an indicator that oscillator "arrays" may not be ideal for energy harvesting while such a distribution of devices does help to increase global vibration control performance.

5. Distributions of SDOF oscillators

In Section 4 it was found that a multitude of SDOF oscillators provided significant vibration suppression primarily at the cost of applying a heavy treatment to the host panel. As a consequence, it was found that, while energy harvesting potential

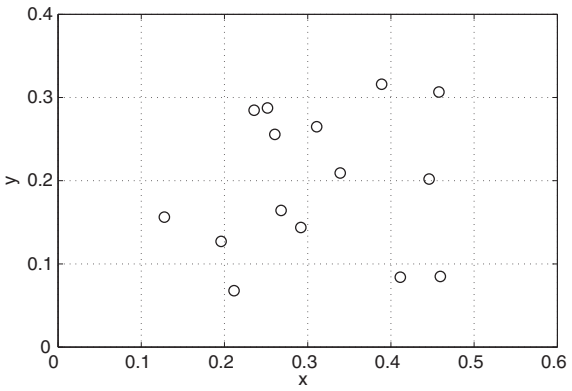

Fig. 5. Randomly selected locations of the 15 oscillators.

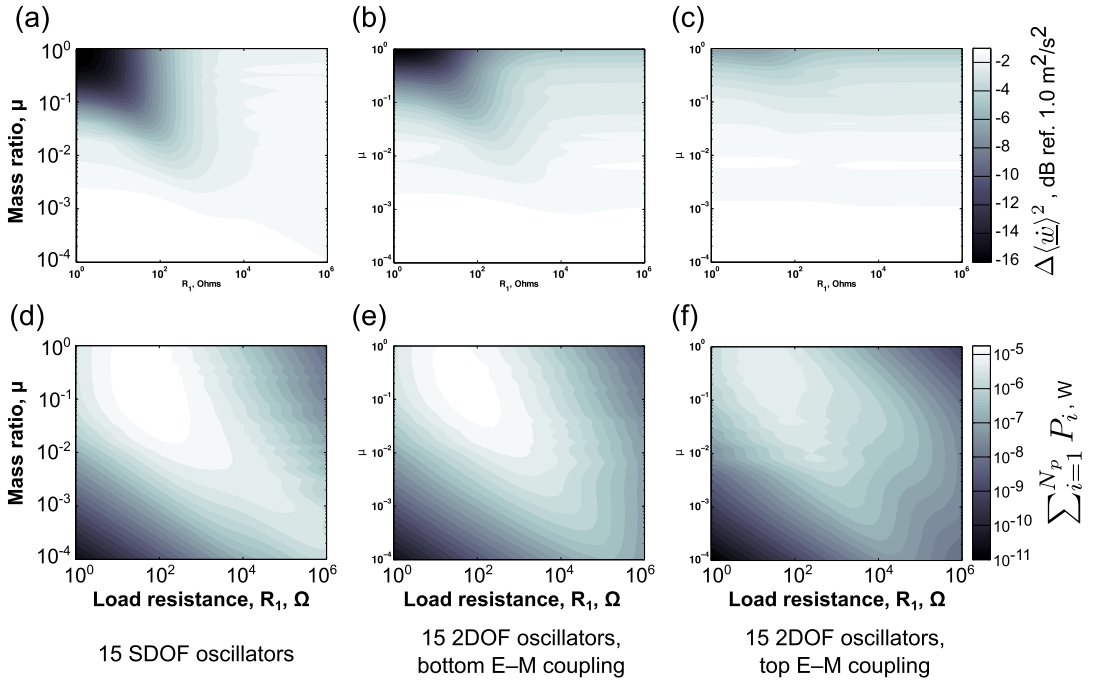

Fig. 6. Vibration suppression for case of the panel having 15 (a) SDOF oscillators, (b) 2DOF oscillators with bottom E–M coupling and (c) 2DOF oscillators having top E–M coupling. Energy harvesting for panel having 15 (d) SDOF oscillators, (e) 2DOF oscillators with bottom coupling and (f) 2DOF oscillators with top coupling.

was maximized close to the same regime of μ as for best vibration suppression, the ability of the array to generate electrical power was less effective than for the single device.

To further explore the concession of numerous oscillators in yielding best simultaneous vibration suppression and net electrical power output, the model was again employed for a variety of μ using $R = 44.6\Omega$, and varying the number of applied devices. Rather than applying the devices in an orderly fashion, a random distribution was utilized, but 50 runs of the model for each value N_p were performed and averaged such that a sufficient combination of positions were explored. For example, using only one model evaluation of a random distribution of $N_p = 2$ would not yield conclusive results; so the average of 50 model evaluations was taken. In the case of $N_p = 1$, the SDOF oscillator was positioned at the panel center.

The results were normalized to data computed for $N_p = 1$ and are presented in Fig. 7. The reduction in panel vibration, Fig. 7(a), is a goal best met using heavy treatments, as several times indicated before. However, it is found that the advantages of increased mass are reduced as the treatment approaches the mass of the host panel. From $\mu = 0.1$ to $\mu = 1$, there is an insignificant improvement in vibration suppression. Distributing this heavier mass amongst a multitude of oscillators does not appear to drastically alter this effect.

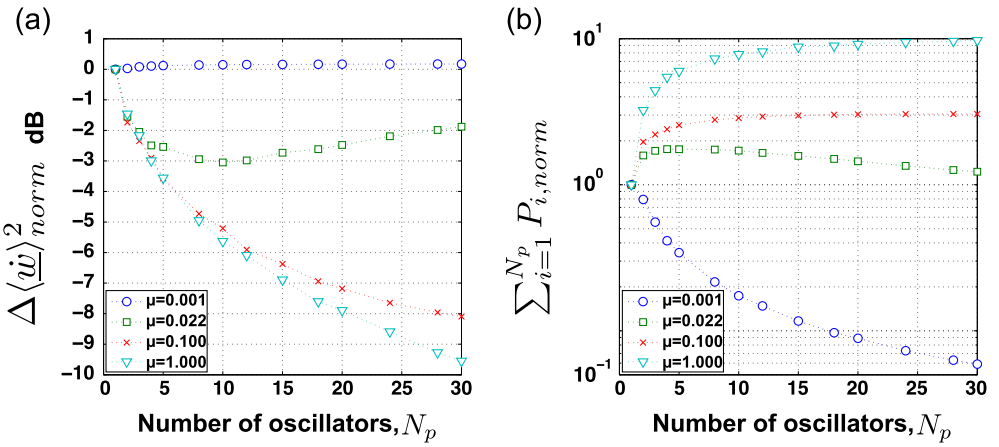

Fig. 7. (a) Average attenuation of mean-square panel velocity. (b) Maximum power output. Data normalized to $N_p = 1$. $R_i = 44.6\Omega$.

Considering more practical mass ratios, $\mu \leqslant 0.1$, the reduction of panel vibration is not necessarily increased using numerous oscillators. In fact, for $\mu = 0.022$ an optimum number is observed, $N_p = 10$. A 3 dB reduction in cumulative mean-square velocity is achieved for this value as compared with the single SDOF oscillator. Distributing the mass amongst an additional number of oscillators decreases the authority of the treatment in passively suppressing the structural vibration suggesting, again, that too many dynamic elements on the host structural ultimately deter each other from their collective performance.

Fig. 7(b) presents the second objective of generating electrical power over the frequency bandwidth of interest. Any increase in the number of oscillators for the very lightweight treatment, $\mu = 0.001$, reduces its potential to convert the absorbed energy to useful electrical power. The heaviest treatment, $\mu = 1$, though seen to increase its power output as N_p increases, ultimately converges to a maximum value, roughly an order of magnitude increase over $N_p = 1$. A similar effect is observed for $\mu = 0.1$, which converges to a maximum power output limit of three times that achievable for a single oscillator. This is the effect observed in Section 4 in finding that the net power output for a given mass ratio does not scale with the array size but indeed is observed to converge to a maximum level.

In contrast, for the treatment of $\mu = 0.022$ a number of oscillators is found to achieve best energy harvesting potential, roughly $4 \leqslant N_p \leqslant 8$. Nearly an increase of two times the power output of $N_p = 1$ is predicted. Since this falls close to the range of optimum N_p which was determined to best improve vibration suppression performance, this serves as evidence that energy harvesting and global vibration attenuation are not always mutually exclusive goals. Proper distribution of the total mass of the treatment amongst a number of oscillators, and best selection of μ, may lead to a condition which maximizes both objectives.

Note that the selection of $\mu = 0.022$ was made in carrying out the simulations as it served as the optimal choice from Fig. 3(d) in achieving maximum energy harvesting from a centrally-positioned SDOF oscillator. Thus, from a practical perspective, optimum μ for energy harvesting purposes may be computed for a given scenario using the present model, and thereafter an optimum array size for the selected μ may be discovered to further increase the power output. It is an interesting twofold benefit that this optimized oscillator array size also corresponds to nearly the same number which provides improved global vibration control.

6. Conclusions

A model of the forced vibration of a host structural panel and attached single- or two-degree-of-freedom electromagnetically-coupled oscillators was employed for the purposes of evaluating the simultaneous goals of global vibration attenuation and maximum energy harvesting. Case studies were considered first of a single oscillator and then for a random distribution of oscillators. In both cases, the 2DOF devices were uniformly less beneficial for the two goals as compared to the SDOF devices.

While the selections of the oscillator mass ratio, μ, and harvesting circuit load resistance, R_1, in maximizing each of the two goals were not identical, it was found that both for single and arrays of oscillators these optimal parameter sets were in relative close proximity. This indicates a feature stated uniquely from the two perspectives of vibration control and energy harvesting. With the prior perspective, it could be said that energy harvesting devices may be effective electromechanical vibration absorbers. From the latter perspective, it could be said that vibration control concerns would make for prime energy harvesting applications with proper device development.

It was observed that the distribution of the oscillator treatment into a number of discrete devices was capable of simultaneously improving both the objectives of vibration attenuation and energy harvesting for small treatment mass ratios, $\mu = 0.022$. When the two objectives are held on equal footing, after selection of μ and R_1, this is an additional parameter flexibility by which to further increase the achievement of both goals.

References

[1] S. Roundy, P.K. Wright, A piezoelectric vibration based generator for wireless electronics, Smart Mater. Struct. 13 (2004) 1131–1142.
[2] H.J. Song, Y.T. Choi, G. Wang, N.M. Wereley, Energy harvesting utilizing single crystal pmn-pt material and application to a self-powered accelerometer, J. Mech. Des. 131 (2009).
[3] A. Erturk, J.M. Renno, D.J. Inman, Modeling of piezoelectric energy harvesting from an l-shaped beam-mass structure with an application to uavs, J. Intell. Mater. Syst. Struct. 20 (2009) 529–544.
[4] C.B. Williams, C. Shearwood, M.A. Harradine, P.H. Mellor, T.S. Birch, R.B. Yates, Development of an electromagnetic micro-generator. Circuits, devices and systems, IEE Proceedings 148 (6) (2001).
[5] R.L. Waters, C. Chisum, H. Jazo, M. Fralick, Development of an electro-magnetic transducer for energy harvesting of kinetic energy and its applicability to a mems-scale device, in: Proceedings of the nanoPower Forum 2008, (2008) pp. 1–6.
[6] P.-H. Wang, X.-H. Dai, D.-M. Fang, X.-L. Zhao, Design, fabrication and performance of a new vibration-based electromagnetic micro power generator, Microelectron. J. 38 (2007) 1175–1180.
[7] B.P. Mann, N.D. Sims, Energy harvesting from the nonlinear oscillations of magnetic levitation, J. Sound Vib. 319 (2009) 515–530.
[8] S.R. Anton, D.J. Inman, Vibration energy harvesting for unmanned air vehicles, in: Smart structures and materials 2008: active and passive smart structures and integrated systems II, Proceedings of SPIE 6928, San Diego, (2008) pp. 1–10.
[9] A. Erturk, W.G.R. Vieira, C. DeMarqui Jr., D.J. Inman, On the energy harvesting potential of piezoaeroelastic systems, Appl. Phys. Lett. 96 (2010).
[10] C.B. Williams, R.B. Yates, Analysis of a micro-electric generator for microsystems, Sens. Actuators A 52 (1996) 8–11.
[11] G. Poulin, E. Sarraute, F. Costa, Generation of electrical energy for portable devices comparative study of an electromagnetic and piezoelectric system, Sens. Actuators A 116 (2004) 461–471.
[12] N.G. Stephen, On energy harvesting from ambient vibration, J. Sound Vib. 293 (2006) 409–425.

[13] N.G. Elvin, N. Lajnef, A.A. Elvin, Feasibility of structural monitoring with vibration powered sensors, Smart Mater. Struct. 15 (2006) 977–986.
[14] J.M. Renno, M.F. Daqaq, D.J. Inman, On the optimal energy harvesting from a vibration source, J. Sound Vib. 320 (2009) 386–405.
[15] G.A. Lesieutre, G.K. Ottman, H.F. Hofmann, Damping as a result of piezoelectric energy harvesting, J. Sound Vib. 269 (2004) 991–1001.
[16] C. De Marqui Junior, A. Erturk, D.J. Inman, Piezoaeroelastic modeling and analysis of a generator wing with continuous and segmented electrodes, J. Intell. Mater. Syst. Struct. 21 (2010) 983–993.
[17] O. Bilgen, Y. Wang, D.J. Inman, Electromechanical comparison of cantilevered beams with multifunctional piezoceramic devices, Mech. Syst. Signal Process. 27 (2012) 763–777.
[18] O. Aldraihem, A. Baz, Energy harvester with a dynamic magnifier, J. Intell. Mater. Syst. Struct. 22 (2011) 521–530.
[19] W. Zhou, G.R. Penamalli, L. Zuo, An efficient vibration energy harvester with a multi-mode dynamic magnifier, Smart Mater. Struct. 21 (2012) 015014.
[20] A. Aladwani, M. Arafa, O. Aldraihem, A. Baz, Cantilevered piezoelectric energy harvester with a dynamic magnifier, J. Vib. Acoust. 134 (2012) 031004.
[21] X. Tang, L. Zuo, Enhanced vibration energy harvesting using dual-mass systems, J. Sound Vib. 330 (21) (2011) 5199–5209.
[22] I.L. Cassidy, J.T. Scruggs, S. Behrens, H.P. Gavin, Design and experimental characterization of an electromagnetic transducer for large-scale vibratory energy harvesting applications, J. Intell. Mater. Syst. Struct. 22 (17) (2011) 2009–2024.
[23] T. Ni, L. Zuo, A. Kareem, Assessment of energy potential and vibration mitigation of regenerative tuned mass dampers on wind excited tall buildings, in: ASME 2011 international design engineering technical conferences & computers and information in engineering conference, Washington DC, 2011.
[24] R.L. Harne, Concurrent attenuation of and energy harvesting from surface vibrations: experimental verification and model validation, Smart Mater. Struct. 21 (2012) 035016.
[25] M. Strasberg, D. Feit, Vibration damping of large structures induced by attached small resonant structures, J. Acoust. Soc. Am. 99 (1) (1995) 335–344.
[26] R.L. Weaver, The effect of an undamped finite degree of freedom fuzzy substructure: numerical solutions and theoretical discussion, J. Acoust. Soc. Am. 100 (5) (1996) 3159–3164.
[27] G. Maidanik, K.J. Becker, Noise control of a master harmonic oscillator coupled to a set of satellite harmonic oscillators, J. Acoust. Soc. Am. 104 (5) (1998) 2628–2637.
[28] I.M. Koç, A. Carcaterra, Z. Xu, A. Akay, Energy sinks: vibration absorption by an optimal set of undamped oscillators, J. Acoust. Soc. Am. 118 (5) (2005) 3031–3042.
[29] L. Zuo, S.A. Nayfeh, Optimization of the individual stiffness and damping parameters in multiple-tuned-mass-damper systems, J. Vib. Acoust. 127 (2005) 77–83.
[30] N.G. Elvin, A.A. Elvin, An experimentally validated electromagnetic energy harvester, J. Sound Vib. 330 (2011) 2314–2324.
[31] K.B. Ocheltree, L.A. Frizzel, Sound field calculation for rectangular sources, IEEE Trans. Ultrason. Ferroelectr. Freq. Control 36 (2) (1989) 242–248.
[32] L.E. Kinsler, A.R. Frey, A.B. Coppens, J.V. Sanders, Fundamentals of Acoustics, fourth edition., Wiley, Hoboken, NJ, 2000.
[33] D.J. Inman, Vibration with Control, first edition., Wiley, Hoboken, NJ, 2006.
[34] T. Aida, K. Kawazoe, S. Toda, Vibration control of plates by plate-type dynamic vibration absorbers, J. Vib. Acoust. 117 (3A) (1995) 332–338.
[35] Y.M. Ram, S. Elhay, The theory of a multi-degree-of-freedom dynamic absorber, J. Sound Vib. 195 (4) (1996) 607–615.
[36] K.V. Singh, Y.M. Ram, Dynamic absorption by passive and active control, J. Vib. Acoust. 122 (2000) 429–433.
[37] L. Zuo, S.A. Nayfeh, Minimax optimization of multi-degree-of-freedom tuned-mass dampers, J. Sound Vib. 272 (2004) 893–908.